Optimum target detection using illuminators of opportunity

Mireille Kubica*, Virginie Kubica*, Xavier Neyt*, Jacques Raout†,
Serge Roques‡, Marc Acheroy*
* Electrical Engineering Dept., Royal Military Academy, Belgium, xavier.neyt@elec.rma.ac.be
† CREA, Ecole de l'Air, Salon de Provence, France, jraout@cr-ea.net
‡ ONERA, Salon de Provence, France, Serge.Roques@onera.fr

***Abstract*— Unlike classical bistatic radars, passive radars make use of illuminators of opportunity to detect targets and to estimate target parameters. One existing radio transmission suitable for passive radar operation is the Global System for Mobile Communication (GSM).**

For non-cooperative bistatic configurations, one of the major difficulties is the estimation of the reference signal which is required to perform detection. This reference signal, a priori unknown, can be extracted from the signal received at the antenna array provided the direction of arrival of the direct path signal is known.

Conventional matched-filter based Doppler filtering offers the possibility of placing the target and interferences in a domain where they can be separated based on Doppler shift. However, slow moving targets residing near mainbeam clutter in the range-Doppler diagram, remain difficult to detect. Internal Clutter Motion (ICM) exacerbates this issue by spreading the clutter signal power in Doppler frequency.

In this paper, we first present a method to estimate autonomously the direction of the illuminating GSM base station from measurements obtained with a two-element antenna array. We passively detect the azimuth of the transmitter without a priori knowledge of the environment. Spatial processing is then employed to attenuate the direct path signal and mitigate its influence on the target detection process.

We then propose two methods able to cope with clutter echoes with non zero-Doppler components. We first propose an extension of a CLEAN-like algorithm. We also propose to extend adaptive matched filters to noise-like signals. The adapted matched filter can be used to suppress strictly static clutter but also clutter affected by ICM.

These methods are validated by using actual clutter measurements obtained from a passive radar using a GSM base station as illuminator of opportunity.

I. Introduction

A passive radar system is a receive-only radar system that does not transmit electromagnetic energy on its own [1]. Instead, it makes use of an illuminator of opportunity already present in the environment as signal source and is thus inherently bistatic. One of the benefits the passive radar can offer is its total undetectability as it contains no transmitter. In this paper, we considered non-cooperative GSM base station illuminators [2], [3]. The GSM system is an interesting resource for passive radar which offers a lot of advantages [4]. One of the benefits of the GSM signals is the digital modulation. This is due to the fact that digital modulated signals in general, and thus GSM signals, exhibit a noise-like behavior since their autocorrelation function resembles a thumbtack. Indeed, the ambiguity function of digital modulated signals exhibit lower sidelobes than the ambiguity function of other type of modulations [5].

The major problem encountered for the detection of ground moving target is the strong direct path signal from the GSM base station and the corresponding ambiguity sidelobes. This is in addition to the surrounding vegetation and buildings that also produce unwanted clutter returns that will seriously degrade the target detection capability. Moreover, vegetation-induced Internal Clutter Motion (ICM) causes a small extension of the clutter signal at non-zero Doppler frequency which will compete with slow moving targets signals.

Furthermore, a central requirement for non-cooperative bistatic radar is the estimation of the direct-path signal used as reference in the coherent processing.

The global processing scheme we considered is shown on figure 1.

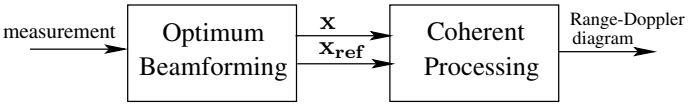

Fig. 1. Processing scheme

The reference signal can be extracted from the signal received at the antenna array provided the direction of arrival of the direct path signal is known. In this paper, we present a method to estimate autonomously the direction of the illuminating GSM base station from measurements obtained with a two-element antenna array. We passively detect the azimuth of the transmitter without a priori knowledge of the environment. Spatial processing is then employed to attenuate the direct path signal and mitigate its influence on the target detection process.

Classical detection involves removal of static clutter returns for instance by using a sidelobe canceler [2]. This removes the major contribution from the clutter and the direct path signal. This step is then typically followed by a range-Doppler matched filtering [6]. However, the Doppler sidelobes of the matched filter will reduce detection performance, in particular in presence of ICM. We propose two methods able to cope with clutter echoes with non zero-Doppler components. The first method is an extension of a CLEAN-like algorithm. We

also propose to extend adaptive matched filters to noise-like signals. The adapted matched filter can be used to suppress strictly static clutter but also clutter affected by ICM.

The paper is organized in the following manner. Section II describes the method to perform an autonomous estimation of the direction of the illuminator of opportunity. Section III presents the separation of the direct path signal and the potential target signal by using optimum beamforming. The section IV discusses the basic echo-canceler. The extension of the CLEAN algorithm is detailed in section V. The section VI reviews the matched filter. The adapted matched filter applied to noise-like signals is detailed in section VII. Finally, in section VIII and IX we present results obtained from real GSM signals. A conclusion is presented in section X

II. Estimation of the direction of the transmitter

Typically, the passive radar system consists of two separate directive antennas which point in different directions [7]–[9]. One antenna points to the target and receives the signal reflected from the target. The other points to the illuminator of opportunity and is used to collect the direct path reference signal neglecting the fact that target signal is also received. Conventional methods to prevent the interception of the direct path signal by the target antenna involve the use of low sidelobe antennas [8] and sidelobe cancellation [9].

We propose a method to perform an autonomous estimation of the direction of the illuminator of opportunity. This presents a considerable operational advantage since the position of the transmitter does not need to be known a priori. Moreover, it makes multistatic operation possible without having to modify the physical setup. The estimation of the direction of the illuminator of opportunity is relatively simple if an array with a large number of elements is used. Due to the lack of degrees of freedom, it is much more challenging when only a two-element array antenna is available.

Various high resolution methods have been proposed to estimate DOA for plane-wave signal incident on an array of sensors [10]. Several of these make assumptions on the signal model. In the following, we propose a maximum likelihood method to estimate the direction of the GSM base station with a two-element array.

The proposed method consists in detecting the maximum of the power spectral density (PSD) based on the Minimum Variance Estimator [11] of the estimated spatial correlation matrix $\widehat{R}$

$$\widehat{P}_{MVE}(\nu_s) = \frac{1}{\mathbf{s}^{\dagger}(\nu_s)\widehat{R}^{-1}\mathbf{s}(\nu_s)} \tag{1}$$

where,

$$\mathbf{s}(\nu_s) = \left[1 \; e^{j2\pi\nu_s} \; e^{j4\pi\nu_s} \; \ldots \; e^{j2\pi(N-1)\nu_s}\right]^T \tag{2}$$

is the spatial steering vector, $\nu_s = \frac{d}{\lambda}\sin(\theta)$ is the normalized spatial frequency corresponding to the DOA θ and d is the distance between two adjacent sensors. N is the number of sensors and λ is the wavelength of the impinging signal. The matrix $\widehat{R}$ will be estimated from the measured data samples by computing the sample covariance matrix. Since a large number of training samples is available, an accurate estimation can be achieved. This estimator represents the angular energy distribution of the received signal. The direction in which the maximum of the PSD is detected is selected as the direction of the transmitter.

III. Separation of the direct path signal from the potential target signal

Once the direction of the illuminator of opportunity is known, the difficulty is to extract a reference signal that would not contain any target echo signals. The presence of target echo signals in the reference signal will lead to ambiguities that will obscure the targets.

Figures 2 and 3 show range-Doppler diagrams after coherent processing with a pure reference signal and a reference signal containing the target signal respectively. These graphs are obtained by using true clutter measurements and by adding an artificial target. Figure 2 depicts the range-Doppler diagram in which the target at the Doppler frequency of $150Hz$ is very prominent. In figure 3, the target signal is attenuated since it is regarded as inherent to the reference signal. Furthermore, symmetrical to the target, an ambiguity due to processing appears in the negative Doppler frequency. These phenomena can make detection difficult or ambiguous. Therefore, the elimination of the target signal in the reference signal is of the highest importance for detection.

To extract the direct path signal, an optimum beamforming is implemented [10], [12]

$$\mathbf{w}_{opt,ref} = \gamma R_{tgt}^{-1}\mathbf{s}(\nu_{Tx}) \tag{3}$$

where γ is a normalization factor, R_{tgt} is the correlation matrix containing the target signal and ν_{Tx} is the normalized spatial frequency corresponding to the direction of the transmitter estimated by the method presented in the previous section. To extract the direct path signal without mismatch, an estimation of the correlation matrix without the reference signal is required. This matrix is not measurable since the reference signal is always present. Thus, the correlation matrix will be synthesized based on a model containing only a target signal and thermal noise.

The direct path reference signal is superimposed with the target echo signals. Target detection will be easier if this direct path signal is attenuated. This problem is solved by using a second filter to suppress the direct path interference by optimally filtering the direct path signal with the filter [10], [12]

$$\mathbf{w}_{opt,tgt} = \gamma R_{Tx}^{-1}\mathbf{s}(\nu) \tag{4}$$

where ν is the potential direction of target, i.e., the direction which gives the smallest ambiguity in the auto-ambiguity function of the reference signal. The correlation matrix R_{Tx} is not known and is synthesized considering a signal arriving from the estimated direction of the interference, the transmitter and thermal noise.

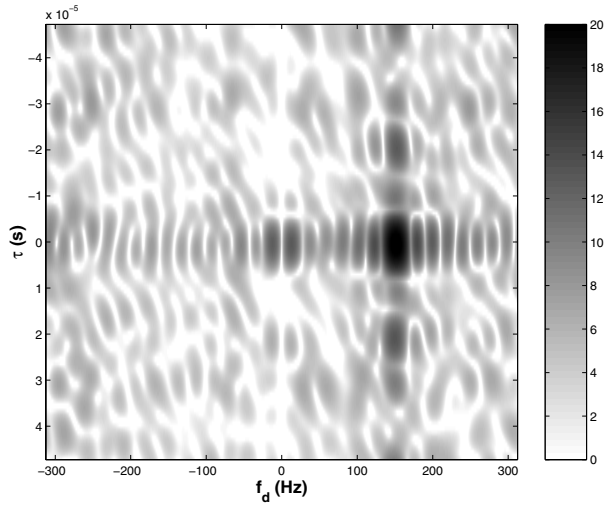

Fig. 2. Range-Doppler diagram obtained with a pure reference signal.

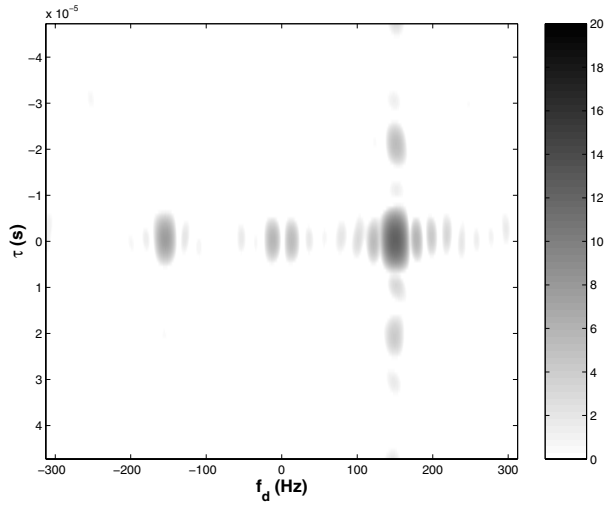

Fig. 3. Range-Doppler diagram obtained with a reference signal containing target signal.

IV. Echo-canceler

A. Principle

An echo-canceler can be used to suppress the direct path signal and static clutter returns in the received signal. The received signal x can be modeled by

$$x(n) = \sum_i a_i x_{ref}(n-\tau_i) + \sum_j b_j x_{ref}(n-\tau_j)e^{-j\omega_j n} \quad (5)$$

with x_{ref} the direct path reference signal, a_i the reflexion coefficient of the clutter patch i with τ_i the corresponding time delay and b_j the reflexion coefficient of the target j with τ_j the corresponding time delay and ω_j its Doppler frequency. x is thus composed of a sum of time delayed versions of the reference signal (static clutter/multipath) and a sum of time-frequency delayed versions of the reference signal (moving targets). To remove static clutter and direct path signal, optimally weighted delayed versions of the direct path reference signal should be subtracted from the received signal x [8]. The optimally weighted delayed versions of the direct path reference signal can be modeled by

$$x_{clutter}(n) = \sum_{i=-K}^{K} \omega_i^* x_{ref}(n-i) \quad (6)$$

We assume that the signal at zero Doppler is (almost) only caused by the direct path signal and the static clutter. We thus neglect the fact that sidelobes of the ambiguity function due to echoes from targets at a non-zero Doppler frequency might also induce some energy at zero Doppler. The echo-canceler can be implemented using a Wiener filter [10] and can thus, under reasonable conditions [10], place a null along the zero Doppler contribution of the clutter and reveal the structure obscured by the ambiguity function sidelobes of the zero-Doppler signals.

However, this classical filtering is not adequate when ICM occurs since it is not able to cope with non-zero Doppler.

B. Application

Figures 5 and 6 show the performance of the echo-canceler. The data used are real signal which contains the echoes of a high-speed train and clutter. The high-speed train (HST) data were acquired in the situation shown on figure 4. Figure 5 shows the range-Doppler diagram before using the echo-canceler. The zero Doppler contribution of the direct path signal and static clutter returns mask the target. In figure 6, the signal energy at zero Doppler was completely suppressed. The peak in the range-Doppler diagram indicates the Doppler frequency of the moving target at $\nu = -0.032\,(-40Hz)$ which corresponds to a velocity of $150km/h$.

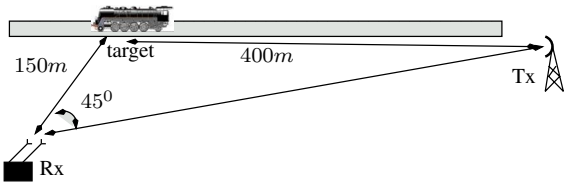

Fig. 4. Situation for the high-speed train data

V. CLEAN algorithm

A. Principle

The echo-canceler algorithm can be reworked as a decomposition of the signal into a basis of non-orthogonal functions, where each basis function is a time-delayed version of the reference signal [13]. We adapted the CLEAN/SCHISM algorithm presented in [14] to noise-like signals by considering time-delayed and frequency-shifted versions of the reference signal as basis functions. This can to some extend be seen as a generalization of echo-cancellation to signals with non-zero Doppler shifts. This last method, although able to decompose the signal quite precisely, can only be used to some extend to filter unwanted signal contributions [14].

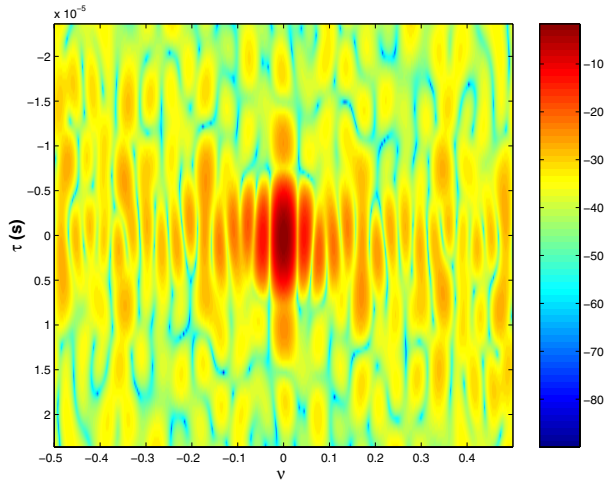

Fig. 5. Range-Doppler diagram of the signal before echo-canceler.

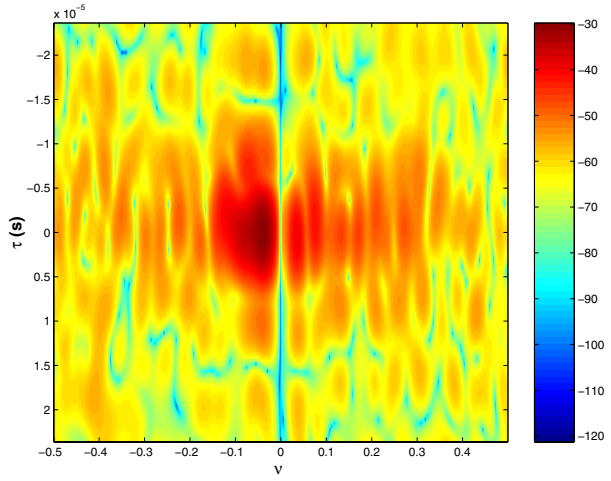

Fig. 6. Range-Doppler diagram of the signal after echo-canceler.

The CLEAN algorithm consists in three steps as illustrated in figure 7. An analysis step where the signal is decomposed in basis functions or modes. At each iteration, the largest contribution of the range-Doppler diagram is found and then a portion of the amplitude of this mode is subtracted. The second step consists in the selection of the modes of interest. (a) Only modes within a Doppler frequency higher than a certain threshold can been kept. (b) The modes which present the most important energy can been conserved. (c) A combination of these two methods can be envisaged. Typically, modes corresponding to low Doppler frequency are left out. Finally, the signal is reconstructed using the selected modes.

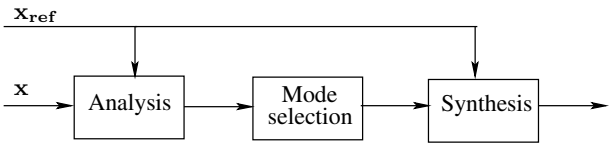

Fig. 7. CLEAN processing schema

B. Interpretation of the basis functions

The CLEAN algorithm finds the frequency and time delay of different contributions but these modes do not necessarily correspond to actual targets. Indeed, two modes corresponding to two different targets, with nearly the same frequency shift can not be discriminated. In this case, CLEAN algorithm will overestimate the amplitude of the basis function. After subtracting out the corresponding basis function, residual lobes will appear. The suppression of non-existing modes could thus generate false alarms.

Figure 8 shows the cross-ambiguity function for a signal which contains two modes with frequency shift of $62.5Hz$ and $68.75Hz$ and amplitude of 7 and 5 respectively. These two modes have not been decomposed and give a total contribution of amplitude 10.14 and frequency shift of $65Hz$. After the first iteration, a second mode with the frequency shift of almost $80Hz$ is detected. This shows that CLEAN modes do not necessarily reveal actual scatterers. This algorithm tends to generate too many false alarms due to these error lobes. These error lobes are directly due to the non orthogonality of the basis functions. Actually, the 2-modes signal is decomposed in many more modes. This illustrates the non linear behavior of the decomposition since the separate decomposition of two signals is not equivalent to the decomposition of both signals together. Moreover, the mode selection process is also another source of non-linearity.

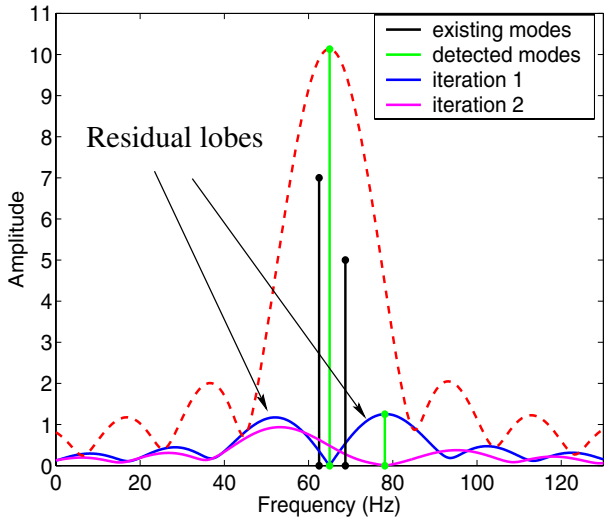

Fig. 8. CLEAN algorithm: detection of non-existing mode.

C. Application

To show the performance of the CLEAN algorithm, we consider 30 iterations which give 30 modes and at each iteration only 0.2 of the amplitude of each mode is removed. We then keep the modes with Doppler frequency above $12Hz$ ($\nu = 0.0096$). Figure 9 shows clearly the negative Doppler frequency of the target's echo.

It should be noted that the contribution of the static clutter and the contributions lower than $12Hz$ ($\nu = 0.0096$) were

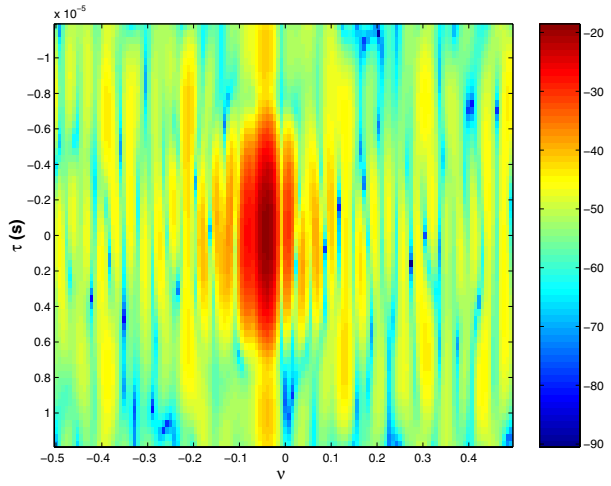

Fig. 9. Range-Doppler diagram after 30 iterations of CLEAN algorithm.

completely suppressed. The residue of the decomposition was not reused in the reconstruction. This corresponds to neglecting scatterers with a small RCS.

VI. Matched filter processing

Target detection is typically performed by computing the correlation between the reference signal and the received echo signals. The generalization of the correlation process is essentially the complex ambiguity function [15]. The ambiguity function corresponds to the matched filter response to the joint time-delay and Doppler shifted version of the reference signal. Because the target's range and relative velocity are unknown, it is necessary to apply a set of filters matched to all possible range-velocity pairs. These matched filters are conjugated time-Doppler shifted versions of the transmitted signal [6]. This bank of filters can be implemented by using the Fourier Transform

$$\chi_{\tau,\nu} = FT\left\{\mathbf{x} \circ \mathbf{x_{ref}}^*(\tau)\right\} \tag{7}$$

where $\mathbf{x_c}(\tau) = \mathbf{x} \circ \mathbf{x_{ref}}^*(\tau)$ is the product of the received signal vector $\mathbf{x}$ and a delayed version of the reference signal vector $\mathbf{x_{ref}}^*$, τ is the time offset and $\circ$ denotes the Hadamar product.

Since the Doppler frequency range that is of interest is much lower than the sampling frequency, the mixed signal $\mathbf{x_c}(\tau)$ can be downsampled as suggested in [15]. Of course, a low-pass filtering has to be performed before the subsampling operation in order to avoid aliasing of noise terms. The influence of this low-pass filter in the Doppler domain is neglected in [15]. This does not impact on detection performance. However, if precise target RCS is to be measured, the attenuation of the low-pass filter should be taken into account.

The use of a matched filter (the Fourier Transform) causes very high sidelobes due to the rectangular window introduced by the finite length of the signal. These sidelobes cause leakage of low-Doppler clutter signal components (due to ICM for instance) not removed by the previous echo-cancellation step. These leakage will in turn hide the signal from low Doppler frequency targets. Of course these sidelobe levels can be reduced by applying a tapering window before computing the Fourier Transform. However, the price to pay for the reduced sidelobes is a broadening of the mainlobe [10]. A broader mainlobe will again obscure slow targets.

VII. Optimum filtering

The matched filtering operation can also be seen as operating directly on the mixed signal $\mathbf{x_c}(\tau)$. Equation (7) can indeed be rewritten as

$$\chi_{\tau,\nu} = \mathbf{w}_{\mathrm{MF}}^{\dagger}\mathbf{x_c}(\tau) \tag{8}$$

where $\mathbf{w}_{\mathrm{MF}} = \left[1\ e^{j2\pi\nu}\ e^{j4\pi\nu}\ \ldots\ e^{j2\pi\nu(M-1)}\right]^T$ is one of the Doppler filters.

We now propose an adapted matched filter to enhance the slow moving target detection capability by reducing the masking effect caused by ICM.

The Adapted Matched Filter can be applied as follows

$$\chi_{\tau,\nu} = \mathbf{w}_{\mathrm{AMF}}^{\dagger}\mathbf{x_c}(\tau) \tag{9}$$

where the scalar $\chi_{\tau,\nu}$ is the output of the filter at the range τ and the frequency ν, and the Adapted Matched Filter $\mathbf{w}_{\mathrm{AMF}}$ is defined by

$$\mathbf{w}_{\mathrm{AMF}} = \gamma R_{i+n}^{-1}\mathbf{s}(\nu) \tag{10}$$

and $\mathbf{s}(\nu)$ is the steering vector at the frequency of interest ν [16]. To compute the Adapted Matched Filter, one needs the interference-plus-noise covariance matrix defined by

$$R_{i+n} = E[\mathbf{x_c}_{i+n}\ \mathbf{x_c}_{i+n}^{\dagger}] \tag{11}$$

where $\mathbf{x_c}_{i+n}$ is a mixed signal assumed to contain the contribution due to interference and noise only. Unlike the matched filter, the adapted matched filter takes the environment into account by using the interference-plus-noise covariance matrix. The adapted matched filter is optimum provided the true covariance matrix is known [10].

This interference rejection requires the estimation and the inversion of an interference-plus-noise covariance matrix. A good overview of the estimation method of the covariance matrix can be found in [17]–[19]. The performance of the AMF will depend on the accuracy of the covariance matrix estimation obtained from real data and can be measured by a SINR loss [18]. Figure 10 compares the SINR loss resulting from different covariance matrix estimation methods.

Four methods are considered. (a) The sample covariance matrix (SCM) with diagonal loading (DL) results from an averaging of the measurements at different ranges. (b) In the principal component (PC) method with diagonal loading (DL) and (c) with covariance matrix taper (CMT), we conserve the dominant modes of the covariance matrix. (d) The theoretical covariance matrix is synthesized with only the interference. The proposed estimation method for this paper is the SCM with diagonal loading. As can be seen on figure 10, the performance of the proposed method is nearly equal to that obtained with the other methods.

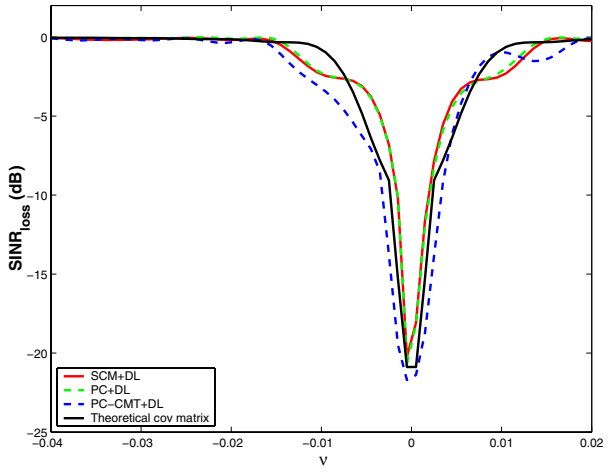

Fig. 10. Comparison of Covariance matrix estimation methods

VIII. Application of the methods

In order to evaluate the performance and capability of the GSM-based passive radar and associated signal processing, experiments were conducted using signals from an operational GSM base station.

A. Echo-canceler and AMF

To illustrate the performance of the algorithm we will compare the results of the processing for two signals : the first signal contains only clutter echoes (including ICM) while the second signal contains in addition a slow-moving target. The clutter signal is obtained from real measurements while the target is simulated.

The block-diagram of the processing steps involved is shown in figure 11.

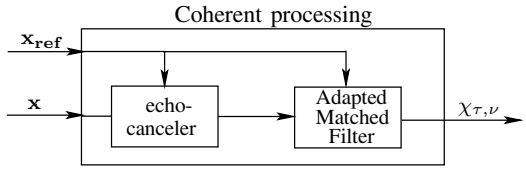

Fig. 11. Block-diagram of the signal processing

We first apply an echo-canceler filter which performs a relatively simple clutter cancellation. The corresponding range-Doppler diagram is shown in figures 12 and 13. As can be seen, the static clutter signal returns was completely suppressed with its ambiguity function sidelobes which could generate too many false alarms. However, strong non-static clutter signal remains, thus hiding the target. These two diagrams do not show any difference although the target is present in the signal of figure 13.

The second step of the algorithm consists in the adapted matched filter which enhances the slow moving target detection capability by reducing the masking effect caused by ICM. The result of the application of the adapted matched filter is shown in figures 14 and 15. The filter indeed attenuates non-static clutter returns in comparison with the classical matched filter of figures 12 and 13. The target now perfectly stands out at $13Hz$ ($\nu = 0.0216$) on figure 15.

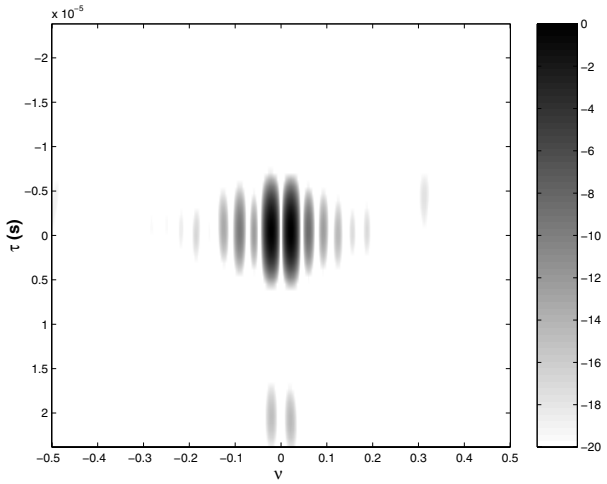

Fig. 12. Range-Doppler diagram of the signal without target after echo-canceler.

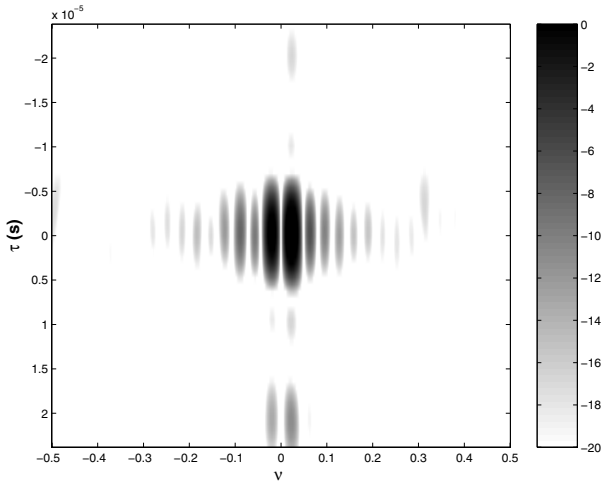

Fig. 13. Range-Doppler diagram of the signal with target after echo-canceler.

Figure 16 shows a cut at $\tau = 0$ in the range-Doppler diagrams of figures 13 and 15. As can be seen, the adapted matched filter indeed attenuates the strong clutter returns at non-zero Doppler thus exposing the target. This result is very revealing and shows the performance of the method.

B. CLEAN algorithm

It is interesting to compare this algorithm with the CLEAN algorithm presented on figure 17.

Figure 18 shows the corresponding range-Doppler diagram. As can be seen, the performance of this second algorithm is excellent and nearly equal to that obtained with the adapted matched filter. The CLEAN algorithm also reveals the presence of the target at $13Hz$ ($\nu = 0.0216$).

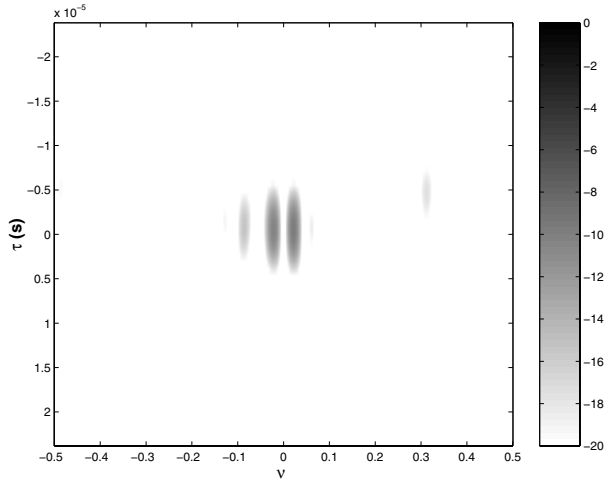

Fig. 14. Range-Doppler diagram of the signal without target after AMF.

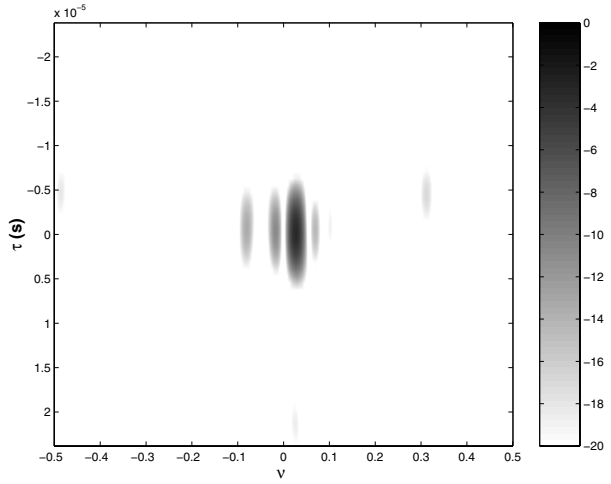

Fig. 15. Range-Doppler diagram of the signal with target after AMF.

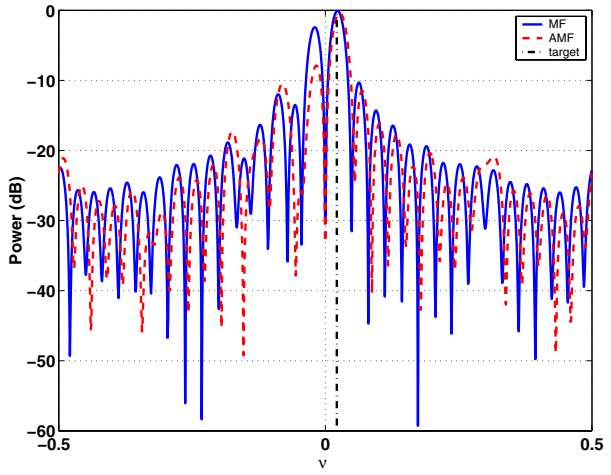

Fig. 16. Cut at $\tau = 0$ in the range-Doppler diagram: MF and AMF comparison after the echo-canceler for the signal with target.

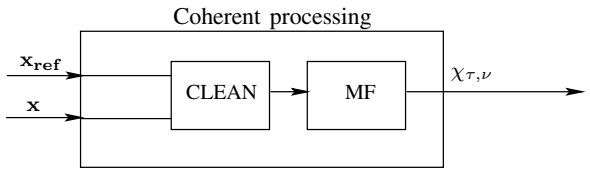

Fig. 17. Block-diagram of the coherent processing with the CLEAN algorithm

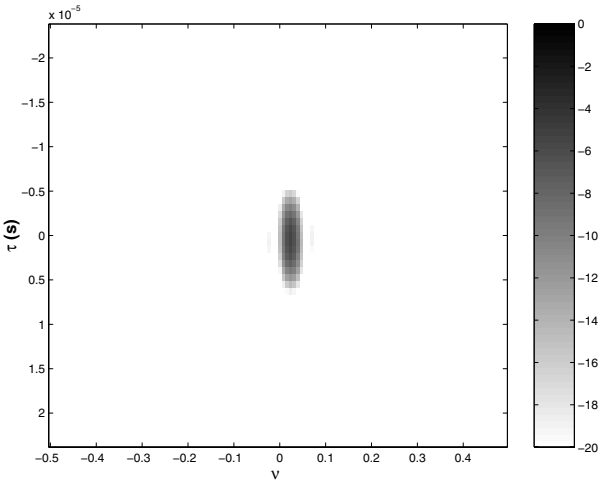

Fig. 18. Range-Doppler diagram of the signal with target after CLEAN.

To compare these two methods in details, a cut at $\tau = 0$ in the range-Doppler diagrams of figure 18 and 15 is necessary. To characterize the performance of these algorithms, we examine the power level of the main lobe and the first secondary lobe on the figure 19. The CLEAN algorithm enables significantly improved detection performance of targets in this scenario in presence of ICM. There is a fundamental difference between these two methods. The adapted matched filter is a linear filter and is optimal among the linear filters. The CLEAN algorithm is non-linear as discussed in section V-B and presents a higher performance than the adapted matched filter when applied to the HST data.

IX. End-to-end results

Once the pure direct path reference signal is separated from the potential target signal, target detection can be implemented by applying a coherent processing. Figure 20 shows a diagram of the signal processing steps. $\mathbf{x}$ and $y(\theta_{tgt}, f_d)$ represent respectively the received signal at the antenna array and the filtered signal after processing.

The measurement considered is the HST data. As can be seen on figure 5, the zero Doppler contribution of the direct path signal and static clutter returns mask the target. The result of the echo-canceler followed by the adapted matched filter can be seen on figure 21. The peak in the range-Doppler diagram clearly indicates the Doppler frequency of the moving target (high-speed train) at $\nu = -0.032$ $(-40Hz)$. This corresponds to a velocity of $150km/h$.

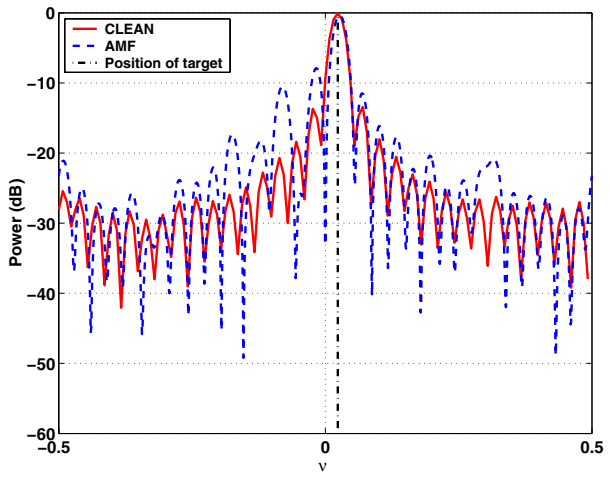

Fig. 19. Cut at $\tau = 0$ in the range-Doppler diagram of the signal with target: AMF and CLEAN algorithm comparison.

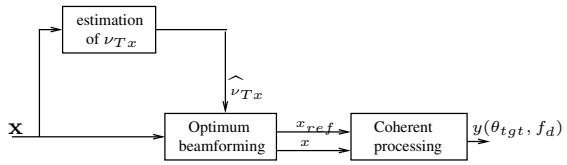

Fig. 20. Signal Processing diagram.

X. Conclusion

This paper first proposes a method to perform an autonomous estimation of the direction of the illuminator of opportunity. Optimum beamforming is then applied to extract the critical reference signal and to provide attenuation of the direct path signal.

An echo-canceler can typically be used to suppress the clutter returns but is not adequate when ICM occurs. The Adapted Matched Filter we propose is shown to be able to detect weak slow moving target echoes when ICM occurs. We also adapted the CLEAN/SCHISM algorithm to noise-like signals which enables significantly improved detection performance of targets in certain scenario's in presence of ICM. The performance of the adapted matched filter and of the CLEAN algorithm are excellent and nearly equal. Experimental results illustrate the ability of the proposed algorithms to perform detection.

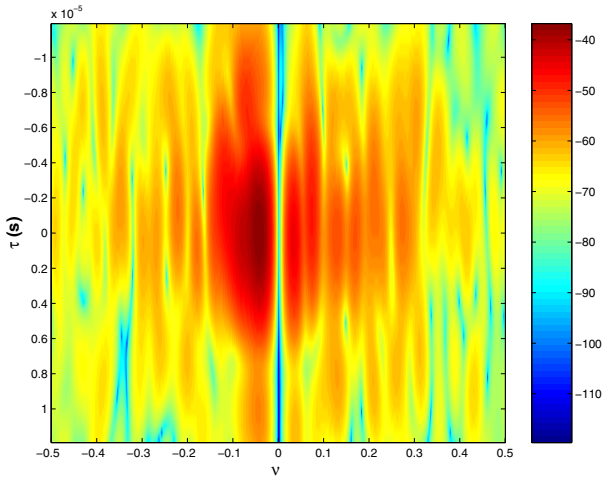

Fig. 21. Range-Doppler diagram observed when the target is detected.

References

[1] H. D. Griffiths, "From a different perspective: Principles, practice and potential of bistatic radar," in *Proceedings of the Radar 2003 conference*, (Adelaide, Australia), Sept. 2003.

[2] H. Sun, D. K. P. Tan, and Y. Lu, "Design and implementation of an experimental gsm based passive radar," *International Conference on Radar*, pp. 418–422, Sept. 2003.

[3] D. K. P. Tan, H. Sun, Y. Lu, and W. Liu, "Feasibility analysis of GSM signal for passive radar," *IEEE Radar Conference*, pp. 425–430, May 2003.

[4] H. D. Griffiths, C. J. Baker, J. Baubert, N. Kitchen, and M. Treagust, "Bistatic radar using satellite-borne illuminators," in *Proc. of RADAR 2002*, pp. 1–5, Oct. 2002.

[5] H. D. Griffiths and C. J. Baker, "Measurement and analysis of ambiguity functions of passive radar transmissions," in *Proceedings of the IEEE Intl. Radar Conference 2005*, pp. 321–325, May 2005.

[6] K. Kulpa, "Continuous wave radars – monostatic, multistatic and network," in *Advances in Sensing with security applications*, (Il Ciocco, Italy), NATO Advanced Study Institute, July 2005.

[7] M. Cherniakov, T. Zeng, and E. Plakidis, "Galileo signal-based bistatic system for avalanche prediction," in *Proceedings of IGARSS 03*, pp. 784–786, July 2003.

[8] D. K. P. Tan, H. Sun, Y. Lui, M. Lesturgie, and H. Chan, "Passive radar using global system for mobile communication signal: theory, implementation and measurements," *IEE Proceedings – Radar, Sonar and Navigation*, vol. 152, pp. 116–123, June 2005.

[9] R. Saini, M. Cherniakov, and V. Lenive, "Direct path interference suppression in bistatic system: DTV based radar," in *Proceedings of the International Radar Conference 2003*, pp. 309–314, Sept. 2003.

[10] D. G. Manolakis, V. K. Ingle, and S. M. Kogon, *Statistical and Adaptive Signal Processing*. USA: McGraw Hill, 1998.

[11] J. Capon, "High-resolution frequency-wavenumber spectrum analysis," *Proceedings of the IEEE*, vol. 57, pp. 1408–1419, Aug. 1969.

[12] J. R. Guerci, *Space-Time Adaptive Processing for Radar*. Norwood, MA: Artech House, 2003.

[13] Z. Czekala and K. S. Kulpa, "Ground clutter suppression in noise radar," in *International Conference on Radar Systems*, (Toulouse, France), Oct. 2004.

[14] G. R. Legters, "Using a plane-wave signal model to suppress airborne GMTI radar clutter and calibrate the array," in *Proceedings of KASSPER 03*, (Las Vegas, NV), pp. 283–288, Apr. 2003.

[15] S. Stein, "Algorithms for ambiguity function processing," *IEEE Transactions on Acoustics, Speech and Signal Processing*, vol. 29, pp. 588–599, June 1981.

[16] L. E. Brennan and L. S. Reed, "Theory of adaptive radar," *IEEE Transactions on Aerospace and Electronic Systems*, vol. 9, pp. 237–252, Mar. 1973.

[17] I. S. Reed, J. D. Mallett, and L. E. Brennan, "Rapid convergence rate in adaptive arrays," *IEEE Transactions on Aerospace and Electronic Systems*, vol. 10, pp. 853–863, Nov. 1974.

[18] R. Klemm, *Principles of space-time adaptive processing*. UK: The Institution of Electrical Engineers (IEE), 2002.

[19] J. R. Guerci and J. S. Bergin, "Principal components, covariance matrix tapers, and the subspace leakage problem," *IEEE Transactions on Aerospace and Electronic Systems*, vol. 38, pp. 152–162, Jan. 2002.